ARTICLE NO. 79-1632R

J80-224

Transonic Flutter Analysis of a Rectangular Wing with Conventional Airfoil Sections

00001
20018
80001

F. E. Eastep* and J. J. Olsen†
Air Force Flight Dynamics Laboratory, Wright-Patterson AFB, Ohio

Flutter analysts have encountered considerable analytical difficulties in the prediction of the flutter stability of aircraft operating in the transonic Mach number regime. Because of the shocks and nonlinearities of transonic flow, the aerodynamic unsteady forces have been difficult to determine and have prohibited accurate determination of the flutter speed. The finite-difference relaxation method is used to determine the oscillatory transonic aerodynamic forces on a uniformly stiff cantilever rectangular wing in a flowfield with mixed subsonic and supersonic regions together with shock waves. The flutter speed is determined at two transonic Mach numbers and is compared to the flutter speed obtained using a classical linear aerodynamic theory.

I. Introduction

THE flutter analyst must insure that a flight vehicle is flutter-free over the entire operating Mach number range, which may include subsonic, transonic, supersonic, and hypersonic speeds. Investigations of the flutter stability of aircraft operating in the transonic regime have encountered considerable analytical difficulties, which have concerned the flutter analyst since the onset of transonic flight. This transonic regime has been identified as the most critical regime for the determination of the flutter stability boundary.[1] Unfortunately, methods to predict transonic oscillatory aerodynamic forces have not existed, so flutter wind tunnel models have been generally used to determine the flutter boundaries in this flight regime. Because of the occurrence of shocks and the inherent nonlinearities associated with the governing equations of transonic flow, the aerodynamic flowfield over an oscillating thin wing has been difficult to define.

Contrary to the investigations at subsonic and supersonic speeds, the flutter stability determination at transonic speeds usually cannot be linearized. As a matter of fact, the governing partial-differential equation from which the aerodynamic forces are to be determined in the vicinity of Mach 1 is nonlinear. Although classical linear unsteady aerodynamic theories for oscillating wings at subsonic[2] and supersonic[3] speeds are well developed, finite-difference methods[4-6] are only beginning to be used to determine the transonic oscillatory aerodynamic forces. The transonic range of flight is particularly critical in flutter prediction, since the transonic effects have prohibited accurate determination of the flutter speed transonic dip with the classical linear methods. The critical transonic dip is depicted in Fig. 1, where the possibility of the flight speed exceeding the flutter speed exists in the transonic region.

Classical linear methods are deficient because the transonic governing equation is nonlinear. The steady thickness, camber, and twist effects must be included in the unsteady analysis, unlike the classical linear methods which allow one to ignore the steady flow in the unsteady analysis. Further, the presence of mixed subsonic and supersonic flow regions, together with the occurrence of shock waves, complicates the determination of the aerodynamic forces on an oscillating wing in a transonic airstream. To define the aerodynamic forces acting on the oscillating wing, we will use the finite-difference relaxation method developed by Farr, Traci, and Albano.[4,5]

Previous transonic flutter analyses have been confined to two-dimensional flow with representative wing sections. This was accomplished to later apply a "strip" representation for aerodynamic forces in the flutter analysis of a wing. Strip analysis is one of common practice in the flutter analysis of wings in subsonic and supersonic airstreams. The present authors, however, felt that in the transonic range, the identification of a section for use with a "strip" flutter analysis would be difficult because of the movement of the location of the shock wave as one moves from one strip to another. In the present analysis, the full three-dimensional flowfield is defined for use in the wing flutter analysis using the computer programs TDSTRN and TDUTRN of Refs. 4 and 5.

Previous investigators have recently begun to use numerical methods for the computation of aerodynamic forces for small-disturbance transonic flows about oscillating airfoils in conjunction with a flutter analysis. In Refs. 4 and 5, Traci et al. performed a flutter analysis for the NACA 64A006 airfoil based on the aerodynamic coefficients computed by using the two-dimensional relaxation finite-difference programs STRANS and UTRANS. The flutter velocities and

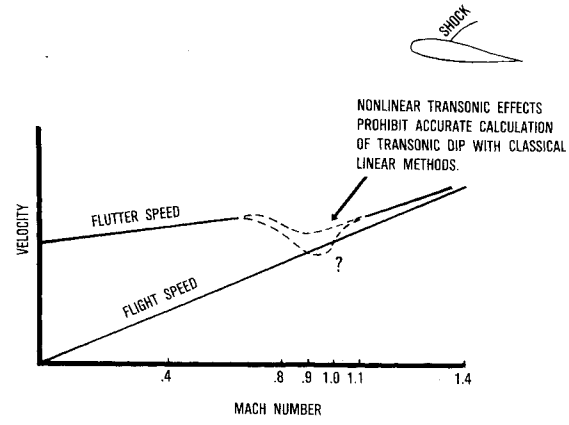

Fig. 1 Typical flutter speed vs Mach number curve of a flight vehicle.

Presented as Paper 79-1632 at the AIAA Atmospheric Flight Dynamics Conference, Boulder, Colo., Aug. 6-8, 1979; submitted Oct. 30, 1979; revision received March 19, 1980. This paper is declared a work of the U.S. Government and therefore is in the public domain.

Index categories: Aerodynamics; Aeroelasticity and Hydroelasticity; Transonic Flow.

*Visiting Scientist, Structures and Dynamics Division. Associate Fellow AIAA.

†Principal Scientist, Analysis and Optimization Branch. Member AIAA.

frequencies were obtained using the "k" method for the airfoil allowed pitching and plunging motion. The results demonstrated the crucial importance of the transonic range by the "dip" in the flutter velocity at a Mach number of 0.85 and the corresponding large variation of flutter frequency in the transonic range. In Ref. 7, Rizzetta presented a flutter analysis of a NACA 64A010 airfoil free to pitch and plunge with steady and oscillatory transonic flows computed using the same relaxation computer programs STRANS and UTRANS. Flutter speeds were obtained for two Mach numbers (0.72 and 0.80) and two angles of attack (0 and 1 deg). He noted the decrease of flutter speed with increasing Mach number and conducted a parameter study of flutter speed with varying frequency ratio and first mass moment. In Ref. 8, Yang et al. compared flutter speed results for both a NACA 64A006 and a NACA 64A010 airfoil using transonic aerodynamic coefficients obtained using the relaxation method (STRANS and UTRANS) and an indicial method (LTRAN2) of Ref. 9. Yang further presented a flutter speed parameter study for various values of airfoil-air mass ratio, frequency ratio, mass center location, and elastic axis location.

In this paper we will perform a flutter analysis at Mach numbers 0.85 and 0.875 of a rectangular wing with constant mass and stiffness properties. The flutter mode will be simply a superposition of fundamental bending and torsion natural modes. The oscillatory transonic aerodynamics will be obtained using the three-dimensional relaxation computer program (TDUTRN) of Refs. 4 and 5. The transonic flutter speed will be determined at two Mach numbers and compared to the speeds obtained using linear aerodynamics.

II. Equations of Motion of a Rectangular Wing

The wing considered for a transonic flutter analysis is the rectangular wing shown in Fig. 2. The structure is modeled as a uniform cantilever beam with constant mass and stiffness along its span. The wing is similar to the wing considered by Goland,[10] but is considerably heavier to insure that the flutter-reduced frequency is in an applicable range for TDUTRN of Refs. 4 and 5.

The equations of motion, considering bending and twisting deformation, are obtained as in Ref. 11:

$$m\frac{\partial^2 w}{\partial t^2} - S\frac{\partial^2 \theta}{\partial t^2} + EI\frac{\partial^4 w}{\partial y^4} = L(y,t) \tag{1}$$

$$I\frac{\partial^2 \theta}{\partial t^2} - S\frac{\partial^2 w}{\partial t^2} - GJ\frac{\partial^2 \theta}{\partial y^2} = M(y,t) \tag{2}$$

where $w(y,t)$ and $\theta(y,t)$ represent the bending and twisting deformations, L and M are the aerodynamic lift and moment per unit span, m is the mass per unit span, S is the first mass moment per unit span, and I is the mass moment of inertia

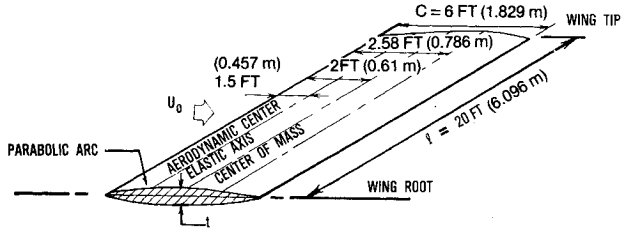

MASS PROPERTIES

M = 11.19 SLUG/FT (534.7 kg/m)
I = 29.145 SLUG FT²/FT (129.5 kg m²/m)
S = 6.705 SLUG FT/FT (97.71 kg m/m)

WING STIFFNESS

EI_b = 23.65 x 10⁶ LB-FT² (9.786 X 10⁶ N m²)
GJ = 2.39 x 10⁶ LB-FT² (0.9890 X 10⁶ N m²)
ω_θ = 23.6677 Hz
ω_β = 11.9025 Hz

Fig. 2 Rectangular wing.

about an elastic axis whose location is shown in Fig. 2. The aerodynamic lift and moment depend upon air density, velocity, wing geometry, and, in a rather complicated manner, on Mach number and reduced frequency.

To obtain the flutter velocity, a modal method is used to represent the flutter mode as a superposition of an assumed bending mode and an assumed twisting mode:

$$w(y,t) = W_R(t) f_w(y) = [\bar{w}e^{i\omega t}][(y/\ell)^2] \tag{3}$$

$$\theta(y,t) = \theta_R(t) f_\theta(y) = [\bar{\theta}e^{i\omega t}][\sin(\pi y/2\ell)] \tag{4}$$

Here ℓ is the semispan of the wing and ω is the circular frequency. The modal assumptions represented by Eqs. (3) and (4) are substituted in the equations of motion, Eqs. (1) and (2), which are satisfied in the Galerkin sense, and result in the following equations after the introduction of artificial structural damping:

$$\ddot{W}_R\int_0^\ell mf_w^2\,dy - \ddot{\theta}_R\int_0^\ell Sf_w f_\theta\,dy + W_R\omega_w^2(1+ig)\int_0^\ell mf_w^2\,dy = \int_0^\ell Lf_w\,dy \tag{5}$$

$$\ddot{\theta}_R\int_0^\ell If_\theta^2\,dy - \ddot{W}_R\int_0^\ell Sf_\theta f_w\,dy + \theta_R\omega_\theta^2(1+ig)\int_0^\ell If_\theta^2\,dy = \int_0^\ell Mf_\theta\,dy \tag{6}$$

where ω_w and ω_θ are the bending and twisting uncoupled frequencies, and g is a structural damping coefficient which has been assumed to be the same for either the bending or twisting mode of deformation. The motion is now assumed to be simple harmonic. The lift and moment can be obtained by superposition of the effects of the bending and twisting deformation as:

$$L = \frac{1}{2}\rho_\infty U_0^2 c\left(C_{L_W}\left(-\frac{\bar{w}}{2b}\right) + C_{L_\theta}\bar{\theta}\right) \tag{7}$$

$$M = \frac{1}{2}\rho_\infty U_0^2 c^2\left(C_{M_W}\left(-\frac{\bar{w}}{2b}\right) + C_{M_\theta}\bar{\theta}\right) \tag{8}$$

where C_{L_W} is the lift coefficient due to bending, C_{L_θ} is the lift coefficient due to twisting, C_{M_W} is the moment coefficient due to bending, and C_{M_θ} is the moment coefficient due to twisting.

This superposition is valid when the governing aerodynamic equations are linear. When the aerodynamic equations are nonlinear, which exists for transonic flow, superposition may only be valid if the unsteady flow is assumed to be a linear perturbation about a nonlinear steady flow. Indeed, this is the assumption made in the numerical computation of the oscillatory transonic flow in TDUTRN and in considering only small bending and twisting deformations. The expressions for lift and moment, Eqs. (7) and (8), are substituted in the equations of motion, Eqs. (5) and (6), which result in the following equations for the bending and twisting of a cantilever wing.

$$\left\{\left(1-(1+ig)\left(\frac{\omega_w}{\omega_\theta}\right)^2\left(\frac{\omega_\theta}{\omega}\right)^2\right)\frac{m}{\pi\rho_\infty b^2}\int_0^1 f_w^2\,dy^* - \frac{1}{2\pi k^2}\int_0^1 C_{L_W}(y^*)f_w\,dy^*\right\}\frac{\bar{w}}{b} - \left\{\frac{S}{\pi\rho_\infty b^3}\int_0^1 f_w f_\theta\,dy^*$$

$$-\frac{1}{\pi k^2}\int_0^1 C_{L_\theta}(y^*)f_W(y^*)\mathrm{d}y^*\Big\}\bar{\theta}=0 \tag{9}$$

$$\left\{\frac{S}{\pi\rho_\infty b^3}\int_0^1 f_w f_\theta \mathrm{d}y^* + \frac{1}{\pi k^2}\int_0^1 C_{M_W}(y^*)f_\theta(y^*)\mathrm{d}y^*\right\}\frac{\bar{w}}{b}$$
$$-\left\{\left(1-(1+ig)\left(\frac{\omega_\theta}{\omega}\right)^2\right)\frac{I}{\pi\rho_\infty b^4}\int_0^1 f_\theta^2\mathrm{d}y^*\right.$$
$$\left.+\frac{2}{\pi k^2}\int_0^1 C_{M_\theta}(y^*)f_\theta(y^*)\mathrm{d}y^*\right\}\bar{\theta}=0 \tag{10}$$

where b is the semichord length and k is reduced frequency equal to $\omega b/U_0$. By defining wing-air mass ratio $\mu=m/\pi\rho_\infty b^2$, location of mass center from the elastic axis $x_\alpha=S/mb$ and radius of gyration $\gamma_\alpha=(I/mb^2)^{1/2}$, Eqs. (9) and (10) can be written in eigenvalue form:

$$\left[\begin{array}{c|c} \int_0^1 f_w^2\mathrm{d}y^* & x_\alpha\int_0^1 f_w f_\theta\mathrm{d}y^* \\ \hline x_\alpha\int_0^1 f_w f_\theta\mathrm{d}y^* & \gamma_\alpha^2\int_0^1 f_w f_\theta^2\mathrm{d}y^* \end{array}\right]$$

$$+\frac{1}{\mu\pi k^2}\left[\begin{array}{c|c} -\frac{1}{2}\int_0^1 C_{L_W}f_w\mathrm{d}y^* & -\int_0^1 C_{L_\theta}f_w\mathrm{d}y^* \\ \hline \int_0^1 C_{M_W}f_\theta\mathrm{d}y^* & 2\int_0^1 C_{M_\theta}f_\theta\mathrm{d}y^* \end{array}\right]\left\{\begin{array}{c} \bar{w}/b \\ \hline -\bar{\theta} \end{array}\right\}$$

$$=\lambda\left[\begin{array}{c|c} (\omega_w/\omega_\theta)^2\int_0^1 f_w^2\mathrm{d}y^* & 0 \\ \hline 0 & \gamma_\alpha^2\int_0^1 f_\theta^2\mathrm{d}y^* \end{array}\right]\left\{\begin{array}{c} \bar{w}/b \\ \hline -\bar{\theta} \end{array}\right\} \tag{11}$$

where the eigenvalue λ is a complex number defined as:

$$\lambda=(1+ig)(\omega_\theta/\omega)^2 \tag{12}$$

At this point of the flutter analysis, if the aerodynamic force and moment can be obtained using a classical linear aerodynamic theory (subsonic or supersonic regime), then the flutter analyst will use the so-called "k" or American method. In this method, various incremental values of reduced frequency and Mach number are selected, which allows one to determine the aerodynamic coefficients of Eq. (11). The corresponding complex eigenvalues, λ, are then obtained from Eq. (11). This process is repeated so that values of g, ω, and U_0 are obtained for each selected reduced frequency. This allows one to obtain $V-g$ and $V-\omega$ diagrams from which the flutter velocity and corresponding flutter frequency can be determined by the condition that the artificial structural damping coefficient g is zero at the flutter velocity. We will also use the "k" method, but the aerodynamic coefficients will be obtained from a numerical computational technique where the flow has mixed subsonic and supersonic regions together with the occurrence of shock waves.

III. Numerical Computation of Transonic Flowfield

The problem of interest is the flow about a planar cantilever wing undergoing bending and twisting deformations and the prediction of oscillatory aerodynamic forces in the transonic speed range. The numerical computation method used for the unsteady flowfield is based on a mixed differencing, line relaxation procedure first formulated by Murman and Cole[12] in their consideration of a thin airfoil in a steady transonic airstream. The procedure was extended by Traci et al.[4,5] to treat the small-disturbance steady and unsteady transonic flows about planar wings. The small-disturbance velocity potential equation can be derived for transonic flow by assuming an inviscid, isentropic flow with only weak shocks existing. A transonic scaling can be introduced so the potential equation for unsteady, small disturbances is written as:

$$(K-\phi_x)\phi_{xx}+\phi_{yy}+\phi_{zz}=2\phi_{xt}+(k/\Omega)\phi_{tt} \tag{13}$$

where ϕ is the transonic-scaled, small-disturbance velocity potential and the transonic scaling parameters are:

$$K=\frac{1-M_\infty^2}{((1+\gamma)\tau M_\infty^2)^{2/3}} \quad \text{and} \quad \Omega=\frac{M_\infty^2}{((1+\gamma)\tau M_\infty^2)^{2/3}}k \tag{14}$$

where τ is the thickness ratio, γ the ratio of specific heats, and k the reduced frequency. Additionally, the boundary conditions must be satisfied as:

$$\phi_y=\frac{\partial f}{\partial x}+\frac{k}{\Omega}\frac{\partial f}{\partial t} \text{ on wing surface} \tag{15}$$

$$\Delta C_p=\phi_x+\frac{k}{\Omega}\phi_t=0 \text{ across wing wake} \tag{16}$$

and

$$\phi_x^2+\phi_y^2+\phi_z^2\to 0 \text{ at great distances from wing} \tag{17}$$

where f is the wing shape function defining the upper and lower wing surfaces. The bending and twisting deformation of the cantilever wing will be assumed to be harmonic boundary disturbances, and the perturbation velocity potential is represented as a steady potential plus a small harmonic disturbance.

$$\phi(x,y,z,t)=\phi^0(x,y,z)+\epsilon\phi^1(x,y,z)e^{i\Omega t} \tag{18}$$

where ϵ is a small parameter giving a measure of the deformation of the cantilever wing. Substituting Eq. (18) into Eq. (13) and neglecting terms of order ϵ^2 and higher, one obtains as coefficients of order 1 and ϵ, the following:

$$(K-\phi_x^0)\phi_{xx}^0+\phi_{yy}^0+\phi_{zz}^0=0 \tag{19}$$

$$(K-\phi_x^0)\phi_{xx}^1+\phi_{yy}^1+\phi_{zz}^1-(\phi_{xx}^0+2i\Omega)\phi_x^1+k\Omega\phi^1=0 \tag{20}$$

Equation (19) can be recognized as the usual transonic nonlinear potential equation for steady flow; whereas, Eq. (20) is a linear, unsteady transonic equation with variable coefficients which depend upon the steady flow velocity potential ϕ^0. Similarly, the expansion of velocity potential and the wing shape function into steady and small oscillatory parts allows one to obtain the appropriate boundary conditions accompanying Eqs. (19) and (20). However, since a numerical computation technique is to be used, the conditions specified in Eq. (17) are approximated by the asymptotic forms given by Newman and Klunker.[13] The line relaxation, finite-difference scheme with the mixed-differencing method allows the numerical solution of Eqs. (19) and (20) together

with the satisfaction of specified boundary conditions. This solution allows one to determine the potential of the mixed (subsonic-supersonic) character of the transonic flowfield. With the velocity potential thus determined, the pressure field and hence the oscillatory pressure difference on the wing can be obtained from

$$C_P = -2(\phi_x + ik\phi) \tag{21}$$

The airfoil sections of the wing will be a 6% thick parabolic arc. The wing is placed at a zero angle of incidence in a transonic airstream with Mach numbers 0.85 and 0.875. The flowfield is to be represented by a rectangular grid array, shown in Fig. 3, which has some 11,600 grid points for the determination of the velocity potential. The interval spacing of the grid array is nonuniform as indicated in Figs. 3a and 3b. The steady, nonlinear transonic flow equation (19) is first solved and then ϕ^0 used in the oscillating linear transonic flow equation (20) for solution of ϕ^1. It is assumed that the shock wave location for oscillatory solution is fixed by the steady solution.

IV. Numerical Results for Aerodynamic Coefficients and Flutter Speed

The nonlinear steady transonic flow potential ϕ^0 is determined at the grid points shown in Fig. 3, while satisfying the boundary conditions imposed on the wing and at the far field. The coefficient of pressure on the upper wing surfaces can be determined from Eq. (21), which allows one to then obtain sectional lift and moment coefficients. The wing to be analyzed is a wing with a 1.83-m (6-ft) chord, a 6.1-m (20-ft) semispan, and an aspect ratio of 3⅓. This wing was placed in a flowfield with Mach numbers of 0.85 and 0.875. Figure 4 depicts variation of the steady pressure on the upper surface along the chord at several span locations for these two Mach numbers. The flow is just barely critical for a Mach number of 0.85, while the shock wave at Mach number of 0.875 has better definition.

The determination of oscillatory lift and moment may now be obtained from the relaxation solution of Eq. (20) using the high-frequency option of TDUTRN computer program of Refs. 4 and 5. Eleven equally spaced wing sections are selected for the determination of section lift and moment about an elastic axis whose location is 0.61 m (2 ft) aft of the wing leading edge. Aerodynamic coefficients were determined for reduced frequencies of 0.0, 0.05, 0.10, 0.15, and 0.20 at the two Mach numbers.

Figure 5 shows real and imaginary parts of pressure coefficient for the values of reduced frequency at several span locations for a twisting deformation. Figure 6 shows the variations of pressure coefficient for a bending deformation. The results shown in Figs. 5 and 6 were obtained for a Mach number of 0.85. The Mach number was increased to 0.875, and the pressures are depicted in Figs. 7 and 8 for, once again, a twisting and bending deformation. Increasing the Mach number caused a rear movement of the shock wave, together with an increase in the coefficient of pressure. For the sake of clarity, only results for reduced frequencies of 0.1 and 0.2 are plotted in Figs. 7 and 8.

The total lift and moment coefficients for both bending and twisting deformations are determined by integrating the differences between pressure coefficients on the upper and lower surfaces over the wing surface. The aerodynamic coefficients associated with bending and twisting deformations are shown in Table 1 for each of the two Mach numbers considered. The increase of Mach number yields the greatest change in C_{M_θ}, the moment coefficient due to a twisting deformation, which would appear to be caused

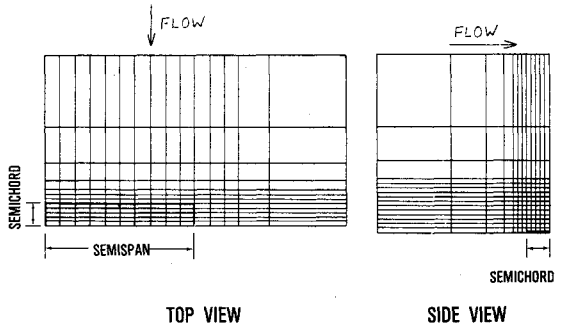

Fig. 3 Rectangular computational grid for TDSTRN and TDUTRN.

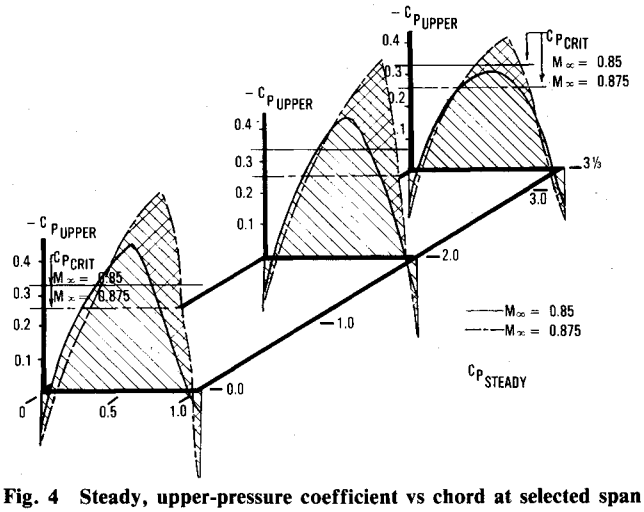

Fig. 4 Steady, upper-pressure coefficient vs chord at selected span stations.

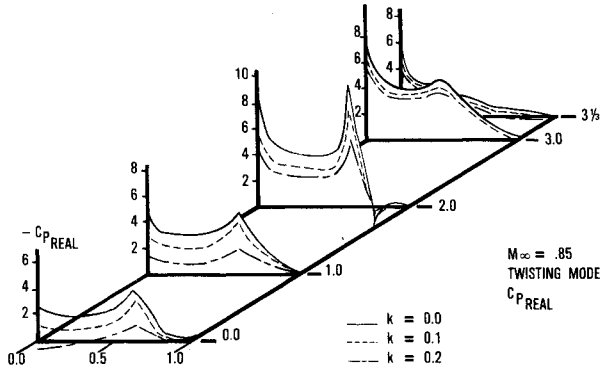

Fig. 5a Pressure coefficient distribution for a rectangular wing oscillating in twist mode, real component, $M_\infty = 0.85$.

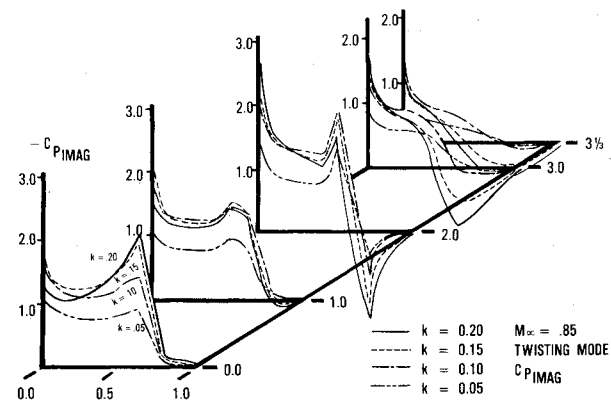

Fig. 5b Pressure coefficient distribution for a rectangular wing oscillating in twist mode, imaginary component, $M_\infty = 0.85$.

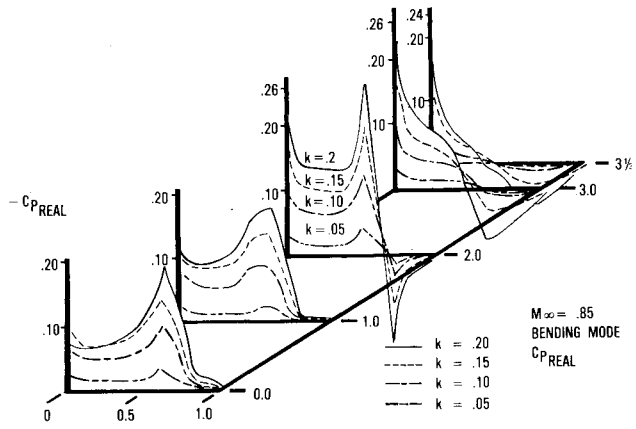

Fig. 6a Pressure coefficient distribution for a rectangular wing oscillating in bending mode, real component, $M_\infty = 0.85$.

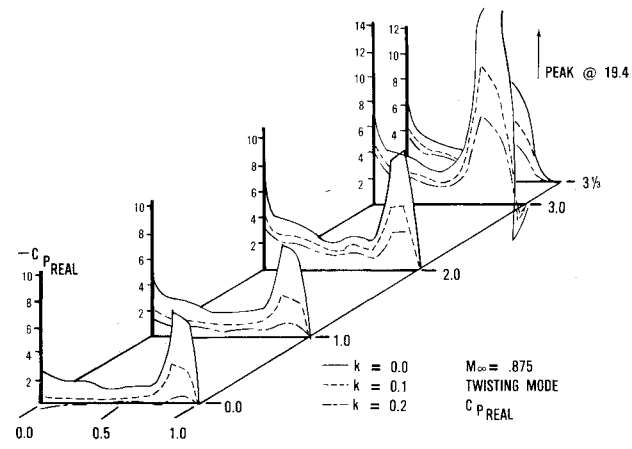

Fig. 7a Pressure coefficient distribution for a rectangular wing oscillating in twist mode, real component, $M_\infty = 0.875$.

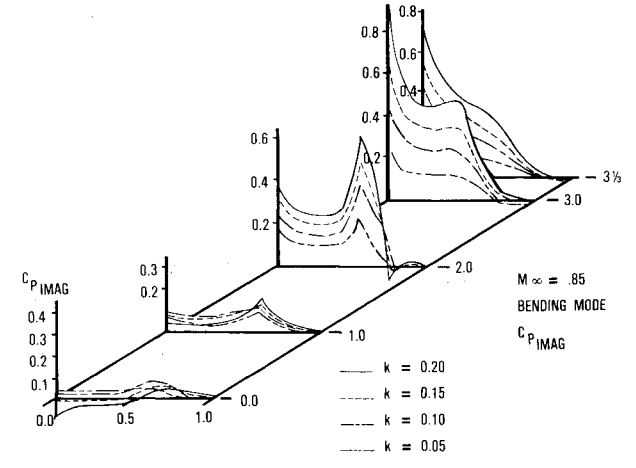

Fig. 6b Pressure coefficient distribution for a rectangular wing oscillating in bending mode, imaginary component, $M_\infty = 0.85$.

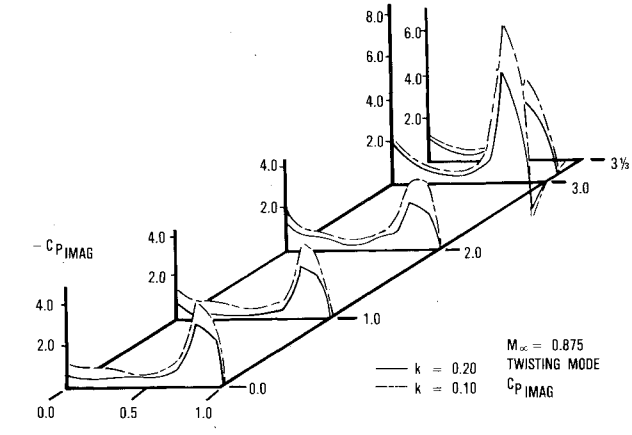

Fig. 7b Pressure coefficient distribution for a rectangular wing oscillating in twist mode, imaginary component, $M_\infty = 0.875$.

Table 1 Total aerodynamic coefficients for a rectangular wing bending and twisting

		Reduced frequency									
		$k=0.0$		$k=0.05$		$k=0.10$		$k=0.15$		$k=0.20$	
Coefficient	M_∞	Real	Imaginary	Real	Imaginary	Real	Imaginary	Real	Imaginary	Real	Imaginary
Twisting											
C_{L_θ}	0.85	19.088	0.0	17.913	−3.355	15.836	−5.070	12.897	−4.618	11.336	−3.952
	0.875	28.208	0.0	23.074	−8.569	16.602	−9.734	12.819	−8.279	10.616	−6.340
C_{M_θ}	0.85	0.248	0.0	0.280	0.149	0.358	0.267	0.288	0.477	0.304	0.619
	0.875	5.993	0.0	4.716	−2.137	3.087	−2.436	2.118	−2.074	1.544	−1.625
Bending											
C_{L_W}	0.85	0.0	0.0	0.084	0.431	0.266	0.728	0.400	0.912	0.471	1.055
	0.875	0.0	0.0	0.244	0.596	0.551	0.819	0.729	0.923	0.764	0.959
C_{M_W}	0.85	0.0	0.0	−0.003	0.003	−0.009	0.007	−0.018	0.011	−0.031	0.015
	0.875	0.0	0.0	0.063	0.125	0.146	0.145	0.201	0.136	0.224	0.098

primarily by the rearward movement of the shock wave together with an increase in shock strength.

In this study, the flutter speed is predicted using the standard "k" method of solution in conjunction with a $V-g$ diagram determined from the complex eigenvalues obtained from the solution of Eqs. (9) and (10) given in Sec. II. Equations (9) and (10) require the evaluation of the integrals of the sectional lift coefficients due to both bending and twisting, weighted with the bending mode f_w, and the section moment coefficients due to bending and twisting weighted with the twisting mode f_θ. These resultant integrals are generally referred to as generalized aerodynamic forces.

The flutter speed of this same cantilever wing is determined using two classical linear aerodynamic theories. The first linear aerodynamic prediction method is a strip analysis used in conjunction with the Theodorsen function[14] corrected for compressibility using a Prandtl-Glauert correction factor. The second linear aerodynamic method used for determining flutter speed is a doublet lattice procedure of Albano and Rodden.[2] The flutter speeds obtained from these two methods are shown in Fig. 9. Also shown in Fig. 9 are the flutter speeds determined at Mach numbers 0.85 and 0.875 using the oscillatory transonic aerodynamic forces obtained using the relaxation finite-difference method. The decrease of

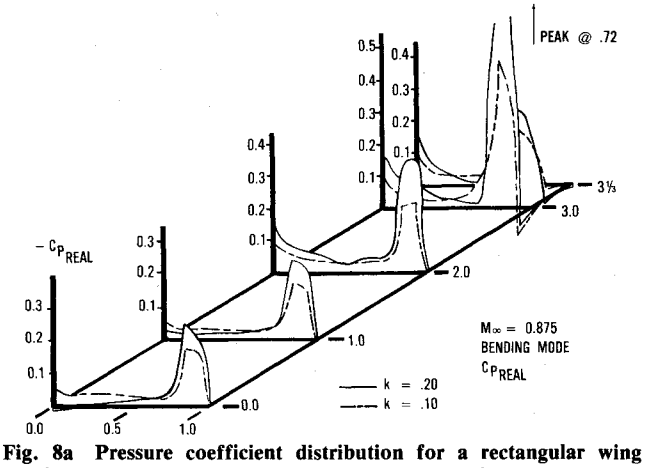

Fig. 8a Pressure coefficient distribution for a rectangular wing oscillating in bending mode, real component, $M_\infty = 0.875$.

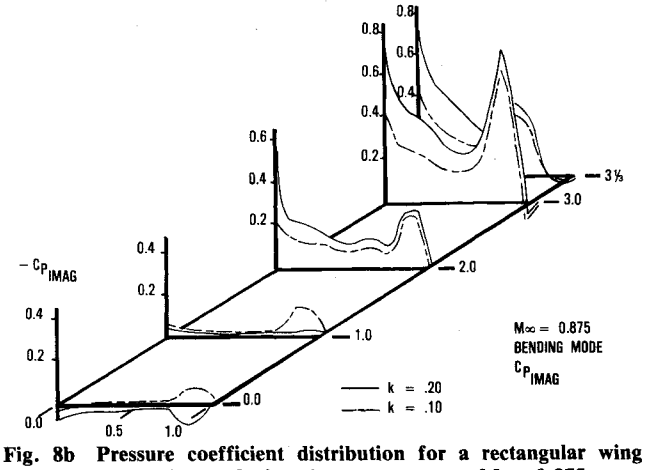

Fig. 8b Pressure coefficient distribution for a rectangular wing oscillating in bending mode, imaginary component, $M_\infty = 0.875$.

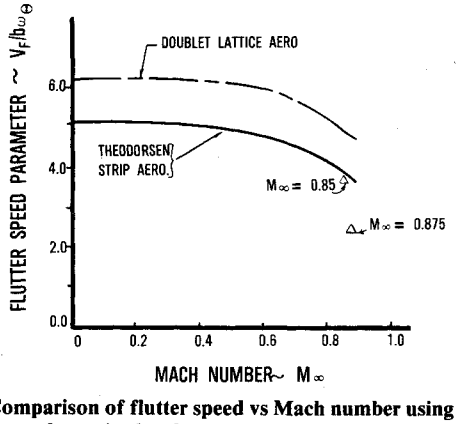

Fig. 9 Comparison of flutter speed vs Mach number using linear and transonic aerodynamics for the rectangular wing ($\mu = 166.28$).

flutter velocity with increasing Mach number is much greater using transonic aerodynamics rather than the two classical aerodynamic theories for the two transonic Mach numbers considered here. A similar reduction occurred for the flutter frequencies obtained using the different aerodynamic prediction methods. Although no flutter speeds were calculated at other Mach numbers using the finite-difference method, it should be noted that at Mach numbers less than 0.7, the flutter speeds should be identical to those obtained using doublet lattice aerodynamics. In Refs. 4 and 5, it is demonstrated that for subcritical flows ($M_\infty \leq 0.7$), the finite-difference, unsteady loads are approximately the same as the unsteady loads obtained using the doublet lattice method of Ref. 2.

V. Concluding Remarks

This paper has used a simple analysis scheme to determine the flutter speed of a rectangular wing in a transonic airstream. The relaxation finite-difference numerical method allows one to introduce the mixed flow regions and fixed shock waves in the flowfield for wing flutter in the "subtransonic" Mach number range. The ability of the structural design engineer to determine structural instabilities over the entire Mach number flight range is enhanced with this flutter prediction technique.

Based on the limited Mach numbers considered, the flutter speed and frequency decreased as the Mach number increased in the transonic range. The decrease in flutter speed was greater when transonic aerodynamics were used rather than linear aerodynamics. Higher Mach numbers must be considered before more general conclusions can be made about transonic flutter. In addition, larger values of reduced frequency must be considered. In this study, the reduced frequencies considered were never higher than 0.2, since convergence was difficult to obtain at high reduced frequencies using TDUTRN.

The representation of the flutter mode by a fundamental bending and torsional mode is a very crude approximation to the actual flutter mode, so that any flutter speed determined, at best, is approximate. To increase the accuracy of the predicted flutter speed, higher bending and torsional modes must be included in the representation of the flutter mode. This would necessitate the computation of the transonic oscillatory aerodynamic loads corresponding to each of the higher modes, which, while not impossible to obtain, would require a substantial amount of more computer time. Further, the flutter speeds obtained here are compared to flutter speeds obtained using classical aerodynamics with the same crude representation of the flutter mode.

References

[1] Mykytow, W. J., "A Brief Overview of Transonic Flutter Problems," AGARD-CP-226, 44th Meeting of AGARD Structures and Materials Panel, Lisbon, Portugal, April 1977.

[2] Albano, E. D. and Rodden, W. P., "A Doublet-Lattice Method for Calculating Lift Distribution on Oscillating Surfaces in Subsonic Flows," *AIAA Journal*, Vol. 7, Feb. 1969, pp. 279-285.

[3] Chipman, R. R., "An Improved Mach-Box Approach for the Calculation of Supersonic Oscillatory Pressure Distributions," *Proceedings of AIAA 17th Structures, Structural Dynamics, and Materials Conference*, King of Prussia, Pa., May 1976.

[4] Traci, R. M., Albano, E. D., and Farr, J. L., "Small Disturbance Transonic Flows About Oscillating Airfoils and Planar Wings," AFFDL-TR-75-100, Aug. 1975.

[5] Farr, J. L., Traci, R. M., and Albano, E. D., "Computer Programs for Calculating Small Disturbance Transonic Flows about Oscillating Planar Wings," AFFDL-TR-75-103, Aug. 1975.

[6] Ehlers, F. E., "A Finite Difference Method for the Solution of the Transonic Flow Around Harmonically Oscillating Wings," NACA CR-2257, July 1974.

[7] Rizzetta, D. P., "Transonic Flutter Analysis of a Two Dimensional Airfoil," AFFDL-TM-77-64, July 1977.

[8] Yang, T. Y., Striz, A. S., and Guruswany, P., "Flutter Analysis of Two-Dimensional and Two-Degree-of-Freedom Airfoils in Small-Disturbance Unsteady Transonic Flow," AFFDL-TR-78-202, Dec. 1978.

[9] Ballhaus, W. F. and Goorgian, P. M., "Computation of Unsteady Transonic Flows by the Indicial Method," *AIAA Journal*, Vol. 16, Feb. 1978, pp. 117-124.

[10] Goland, M., "The Flutter of a Uniform Cantilever Wing," *Journal of Applied Mechanics*, Vol. 12, No. 4, Dec. 1945.

[11] Bisplinghoff, R. L., Ashley, H., and Halfman, R. L., *Aeroelasticity*, Addison-Wesley, Reading, Mass., 1955, pp. 555-568.

[12] Murman, E. M. and Cole, J. D., "Calculation of Plane Steady Transonic Flows," *AIAA Journal*, Vol. 9. Jan. 1971, pp. 114-121.

[13] Newman, P. A. and Klunker, E. B., "Computation of Transonic Flow about Finite Lifting Wings," *AIAA Journal*, Vol. 10, July 1972, pp. 971-973.

[14] Smilg, B. and Wasserman, L. S., "Application of Three-Dimensional Flutter Theory to Aircraft Structures," Army Air Force Tech. Rept. 4798, July 1942.